CHAPTER 2

STUDY OF THE DISPERSION CHARACTERISTICS OF A HEXAGONAL PHOTONIC CRYSTAL FIBER

In this chapter, a solid core photonic crystal fiber (PCF) with hexagonal lattice of air holes is proposed and numerically investigated. Chromatic dispersion and normalized frequency (V_{eff}) parameters are calculated for the PCF with the help of frequency domain algorithm based on finite difference time domain (FDTD) method. Also effective refractive index has been calculated in case of polarized as well as scalar input field. The refractive index of the core of the PCF is varied from 1.45 to 1.48 in order of 0.01 and effects on the different parameters are observed in a figurative manner. We see that negative dispersion has been achieved for each refractive index of the core in the S+C+L communication bands. Flattened dispersion is attained for diameter of air hole to pitch ratio (d/Λ) equal to 0.78 in the same band. When increment is done in the refractive index of the core of PCF, the values of V_{eff} plotted against wavelength also increase.

2.1 GENERAL

There is a need of dispersion compensation in a long-distance optical data communication system because the input pulse broadens as it moves along the fiber and the data gets affected. Dispersion compensating fibers (DCFs) [111] are just the right candidates for minimizing the dispersion attained in the conventional fibers used for communication. Photonic crystal fiber (PCF) [112] has the ability to act as a prominent DCF due to the flexibility being offered at the time of designing of PCF. Initially Birks et

al. [39] gave the idea of using PCF as a dispersion compensator. In continuity a lot of people worked upon PCF for its dispersion compensating ability. Work on dispersion compensation over the S+C+L+U communication bands was presented by M. Franco et al. [82]. D.C. Tee et al. [84] presented a PCF which exhibits very high negative dispersion in all the telecommunication wavebands. The design parameters of a PCF include air hole diameter (d), distance between center of two consecutive air-holes also known as pitch (Λ) and number of rings of air holes in the cladding. The air holes in the cladding can be arranged in a hexagonal, circular or square configuration. It is always desired that a particular PCF is manufactured such that it shows an ultra-flattened large negative dispersion to be used in an optical communication system. For reduction in insertion loss and cost of installation, PCF should be smaller in length with the ability to compensate high positive dispersion.

An important parameter related to PCF is its normalized frequency (V_{eff}), the value of which determines the number of modes that can propagate in a PCF. The unique property of PCF is, it can operate in single mode as well as multimode phenomena. The design of PCF based on normalized frequency has been explained by M. Nielsen et al. [47] in their work published in the year 2003. Analysis of cut-off conditions for mode propagation along with normalized frequency in PCF is conducted by N. A. Mortensen et al. [37]. V_{eff} is calculated and plotted against wavelength for single mode operation of PCF as a part of their work in [114].

The polarization properties of PCF are also an important feature, which increases the spectrum of applications of PCF. Birefringence (B) and dispersion parameters have been computed, taking into consideration the polarization behaviour of an elliptical PCF by

[115]. High birefringence has been obtained and represented accompanying with graph of effective index versus wavelength for a PCF structure by T. P. Hansen et al [87]. The recent works on PCF mostly emphasize on the evaluation of the birefringence parameter for different geometries of PCF [115].

2.2 THEORETICAL METHOD

There are several methods to study the different properties of a PCF which include finite element method (FEM), plane wave expansion (PWE), multi pole method (MPM), beam propagation method (BPM) and finite difference time domain (FDTD) technique. FEM and FDTD are much sought out methods among all as FEM is easier to implement whereas FDTD is more accurate.

To start finding effective index, we have taken a vectorial wave equation of the form as given below:

$$\nabla^2 E + \nabla\left(\frac{\nabla \varepsilon_{(x,y)}}{e_{(x,y)}} \cdot E\right) + k_0^2 \varepsilon_{(x,y)} E = 0 \tag{2.1}$$

Now, let us consider a structure uniform in the z direction. In this case, the derivative of relative permittivity with respect to z is zero:

$$\frac{\partial \varepsilon_{(x,y)}}{\partial z} = 0 \tag{2.2}$$

Thus, the second term in Equation (2.1) can be written as

-

$$\nabla\left(\frac{\nabla \varepsilon_{(x,y)}}{\varepsilon_{(x,y)}} \cdot E\right) = \nabla\left(\frac{1}{\varepsilon_{(x,y)}} \frac{\partial \varepsilon_{(x,y)}}{\partial x} E_X + \frac{1}{\varepsilon_{(x,y)}} \frac{\partial \varepsilon_{(x,y)}}{\partial y} E_y\right) \tag{2.3}$$

After substituting Equation (2.3) into Equation (2.1), we separate Equation (2.1) into the x and y components. Thus, we acquire the vectorial wave equation using the electric field components E_X and E_y. Its x component is -

$$\frac{\partial^2 E_X}{\partial x^2} + \frac{\partial}{\partial x}\left(\frac{1}{\varepsilon_{(x,y)}}\frac{\partial \varepsilon_{(x,y)}}{\partial x}E_X\right) + \frac{\partial^2 E_X}{\partial y^2} + \frac{\partial^2 E_X}{\partial z^2} + k_0^2 \varepsilon_{(x,y)} E_X + \frac{\partial}{\partial x}\left(\frac{1}{\varepsilon_{(x,y)}}\frac{\partial \varepsilon_{(x,y)}}{\partial y}E_y\right) = 0 \qquad (2.4)$$

and its y component is

$$\frac{\partial^2 E_y}{\partial x^2} + \frac{\partial^2 E_y}{\partial y^2} + \frac{\partial}{\partial y}\left(\frac{1}{\varepsilon_{(x,y)}}\frac{\partial \varepsilon_{(x,y)}}{\partial y}E_y\right) + \frac{\partial^2 E_y}{\partial z^2} + k_0^2 \varepsilon_{(x,y)} E_y + \frac{\partial}{\partial y}\left(\frac{1}{\varepsilon_{(x,y)}}\frac{\partial \varepsilon_{(x,y)}}{\partial x}E_x\right) = 0 \qquad (2.5)$$

Now because

$$\frac{\partial}{\partial x}\left\{\frac{1}{\varepsilon_{(x,y)}}\frac{\partial}{\partial x}(\varepsilon_{(x,y)}E_x)\right\} = \frac{\partial^2 E_x}{\partial x^2} + \frac{\partial}{\partial x}\left(\frac{1}{\varepsilon_{(x,y)}}\frac{\partial \varepsilon_{(x,y)}}{\partial x}E_x\right) \qquad (2.6)$$

and

$$\frac{\partial}{\partial y}\left\{\frac{1}{\varepsilon_{(x,y)}}\frac{\partial}{\partial y}(\varepsilon_{(x,y)}E_y)\right\} = \frac{\partial^2 E_y}{\partial y^2} + \frac{\partial}{\partial y}\left(\frac{1}{\varepsilon_{(x,y)}}\frac{\partial \varepsilon_{(x,y)}}{\partial y}E_y\right) \qquad (2.7)$$

where β is the propagation constant. Thus, using Equations (2.4) and (2.5), we obtain for the x component -

$$\frac{\partial^2 E_X}{\partial x^2} + \frac{\partial}{\partial x}\left(\frac{1}{\varepsilon_{(x,y)}}\frac{\partial \varepsilon_{(x,y)}}{\partial x}E_X\right) + \frac{\partial^2 E_X}{\partial y^2} + (k_0^2 \varepsilon_{(x,y)} - \beta^2)E_X + \frac{\partial}{\partial x}\left(\frac{1}{\varepsilon_{(x,y)}}\frac{\partial \varepsilon_{(x,y)}}{\partial y}E_y\right) = 0 \qquad (2.8)$$

and for the y component -

$$\frac{\partial^2 E_y}{\partial x^2} + \frac{\partial^2 E_y}{\partial y^2} + \frac{\partial}{\partial y}\left(\frac{1}{\varepsilon_{(x,y)}}\frac{\partial \varepsilon_{(x,y)}}{\partial y}E_y\right) + (k_0^2 \varepsilon_{(x,y)} - \beta^2)E_y + \frac{\partial}{\partial y}\left(\frac{1}{\varepsilon_{(x,y)}}\frac{\partial \varepsilon_{(x,y)}}{\partial x}E_x\right) = 0 \qquad (2.9)$$

In the equations of fields that transmits in optical waveguides, the expression complementary to the interaction between the x-directed electric field component E_X and the y-directed electric field component E_y can be written as :

$\frac{\partial}{\partial x}\left(\frac{1}{\varepsilon_r}\frac{\partial \varepsilon_r}{\partial y}E_y\right)$ and $\frac{\partial}{\partial y}\left(\frac{1}{\varepsilon_r}\frac{\partial \varepsilon_r}{\partial x}E_x\right)$ from Equations (2.8) and (2.9).

Since these terms are small, skipping these terms for the effect, we can separate the vectorial wave equations for the *x*- and y-directed field components and minimize them to semi-vectorial wave equations. In the designing of optical waveguide devices, semi-vectorial investigation by ignoring the terms for interaction are widely used, in which the coupling between x-and y-directed polarizations does not have to be taken into consideration.

The electric field component E_y is assumed to be zero in case of a quasi-TE mode, where the main component of the electric field representation is the electric field component E_x in the x-direction. So according to Equation (2.8), the semivectorial wave equation for the quasi-TE mode can be written as:

$$\frac{\partial^2 E_x}{\partial x^2}+\frac{\partial}{\partial x}\left(\frac{1}{\varepsilon_{(x,y)}}\frac{\partial \varepsilon_{(x,y)}}{\partial x}E_X\right)+\frac{\partial^2 E_X}{\partial y^2}+(k_0^2\varepsilon_{(x,y)}-\beta^2)E_x=0 \qquad (2.10)$$

which, can further be rewritten as :

$$\frac{\partial}{\partial x}\left\{\frac{1}{\varepsilon_{(x,y)}}\frac{\partial}{\partial x}(\varepsilon_{(x,y)}E_x)\right\}+\frac{\partial^2 E_X}{\partial y^2}+(k_0^2\varepsilon_{(x,y)}-\beta^2)E_X=0 \qquad (2.11)$$

The E_x representation of wave equation derived for the quasi-TE mode is -

$$\frac{\partial^2 E_x}{\partial x^2} + \frac{\partial}{\partial x}\left(\frac{1}{\varepsilon_r}\frac{\partial \varepsilon_r}{\partial x}E_x\right) + \frac{\partial^2 E_x}{\psi^2} + (k_0^2\varepsilon_r - \beta^2)E_X = 0 \qquad (2.12)$$

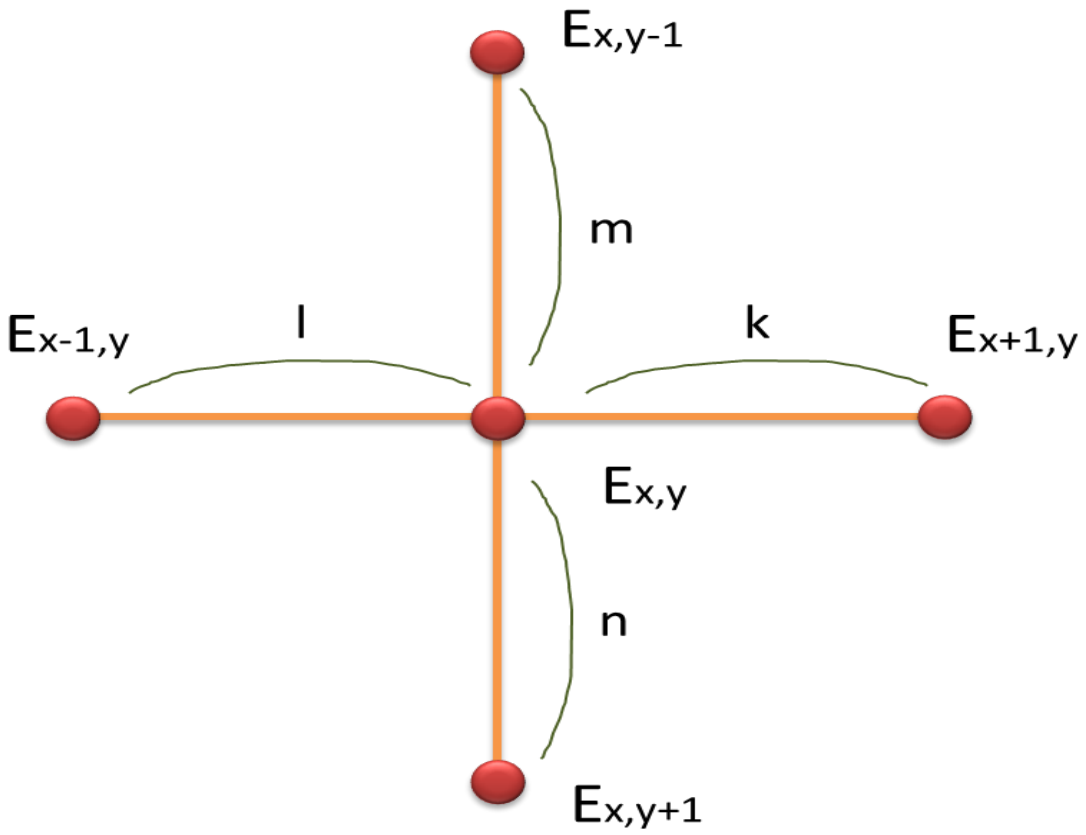

Figure 2.1 Non-equidistant discretization for the finite-difference method.

Now we have to obtain the finite-difference expression for the above equation. The transverse distribution of field for non-discretized PCF structure for the implementation of finite difference technique has been shown in Figure 2.1.

Using for $E_{i+1,j}, E_{i-1,j}, E_{i,j+1}$, and $E_{i,j-1}$, Taylor series expansions around (i,j), we get

$$E_{i+1,j} = E_{i,j} + \frac{1}{1!}\frac{\partial E}{\partial x}|_{i,j} \cdot k + \frac{1}{2!}\frac{\partial^2 E}{\partial x^2}|_{i,j} \cdot k^2 + O(k^3) \qquad (2.13)$$

$$E_{i-1,j} = E_{i,j} - \frac{1}{1!}\frac{\partial E}{\partial x}|_{i,j} \cdot l + \frac{1}{2!}\frac{\partial^2 E}{\partial x^2}|_{i,j} \cdot w^2 + O(l^3) \tag{2.14}$$

$$E_{i,j+1} = E_{i,j} + \frac{1}{1!}\frac{\partial E}{\partial y}|_{i,j} \cdot n + \frac{1}{2!}\frac{\partial^2 E}{\Phi^2}|_{i,j} \cdot n^2 + O(n^3) \tag{2.15}$$

$$E_{i,j-1} = E_{i,j} - \frac{1}{1!}\frac{\partial E}{\partial y}|_{i,j} \cdot m + \frac{1}{2!}\frac{\partial^2 E}{\partial y^2}|_{i,j} \cdot m^2 + O(m^3) \tag{2.16}$$

Calculating finite difference of each term of the Equation 2.12, we get a bit long relation as below:

$$\begin{aligned}
&\frac{2}{k(k+l)}E_{i+1,j} + \frac{2}{l(k+l)}E_{i-1,j} - \frac{2}{\mathrm{kl}}E_{i,j} + \frac{2}{k+l} \\
&\times \{\frac{1}{k}\frac{\varepsilon_r(i+1,j) - \varepsilon_r(i,j)}{\varepsilon_r(i+1,j) + \varepsilon_r(i,j)}(E_{i+1,j} + E_{i,j}) \\
&-\frac{1}{l}\frac{\varepsilon_r(i,j) - \varepsilon_r(p-1,q)}{\varepsilon_r(i,j) + \varepsilon_r(i-1,j)}(E_{i,j} + E_{i-1,j})\} \\
&+\frac{2}{n(n+m)}E_{i,j+1} + \frac{2}{m(n+m)}E_{i,j-1} - \frac{2}{\mathrm{mn}}E_{i,j} + \{k_0^2\varepsilon_r(i,j) - \beta^2\}E_{i,j} \\
&= \frac{2}{l(k+l)}\{1 - \frac{\varepsilon_r(i,j) - \varepsilon_r(i-1,j)}{\varepsilon_r(i,j) + \varepsilon_r(i-1,j)}\}E_{i-1,j} \\
&+\frac{2}{k(k+l)}\{1 - \frac{\varepsilon_r(i,j) - \varepsilon_r(i+1,j)}{\varepsilon_r(i,j) + \varepsilon_r(i+1,j)}\}E_{i+1,j} \\
&+\{-\frac{2}{\mathrm{kl}} - \frac{2}{l(k+l)}\frac{\varepsilon_r(i,j) - \varepsilon_r(i-1,j)}{\varepsilon_r(i,j) + \varepsilon_r(i-1,j)} \\
&-\frac{2}{k(k+l)}\frac{\varepsilon_r(i,j) - \varepsilon_r(i+1,j)}{\varepsilon_r(i,j) + \varepsilon_r(i+1,j)}E_{i,j}
\end{aligned}$$

$$+\frac{2}{m(n+m)}E_{i,j-1}+\frac{2}{n(n+m)}E_{i,j+1}-\frac{1}{\mathrm{nm}}E_{i,j}+\{k_0^2\varepsilon_r(i,j)-\beta^2\}E_{i,j}$$
$$=\frac{2}{l(k+l)}\frac{2\varepsilon_r(i-1,j)}{\varepsilon_r(i,j)+\varepsilon_r(i-1,j)}E_{i-1,j}$$
$$+\frac{2}{k(k+l)}\frac{2\varepsilon_r(i+1,j)}{\varepsilon_r(i,j)+\varepsilon_r(i+1,j)}E_{i+1,j}$$
$$+\{-\frac{2}{\mathrm{kl}}-\frac{2}{l(k+l)}\frac{\varepsilon_r(i,j)-\varepsilon_r(i-1,j)}{\varepsilon_r(i,j)+\varepsilon_r(i-1,j)}$$
$$-\frac{2}{k(k+l)}\frac{\varepsilon_r(i,j)-\varepsilon_r(i+1,j)}{\varepsilon_r(i,j)+\varepsilon_r(i+1,j)}E_{i,j}$$
$$+\frac{2}{m(n+m)}E_{i,j-1}+\frac{2}{m(n+m)}E_{i,j+1}-\frac{1}{\mathrm{nm}}E_{i,j}$$
$$+\{k_0^2\varepsilon_r(i,j)-\beta^2\}E_{i,j}=0 \tag{2.17}$$

Converting the above relation into a simpler form, finite difference expression of Equation 2.12 can be written as:

$$\alpha_l E_{i-1,j}+\alpha_k E_{i+1,j}+\alpha_m E_{i,j-1}+\alpha_n E_{i,j+1}$$
$$+(\alpha_x+\alpha_y)E_{i,j}+\{k_0^2\varepsilon_r(i,j)-\beta^2\}E_{i,j}=0 \tag{2.18}$$

where

$$\alpha_l=\frac{2}{l(k+l)}\frac{2\varepsilon_r(i-1,j)}{\varepsilon_r(i,j)+\varepsilon_r(i-1,j)} \tag{2.19}$$

$$\alpha_k=\frac{2}{k(k+l)}\frac{2\varepsilon_r(i+1,j)}{\varepsilon_r(i,j)+\varepsilon_r(i+1,j)} \tag{2.20}$$

$$\alpha_m=\frac{2}{m(m+n)} \tag{2.21}$$

$$\alpha_n=\frac{2}{n(m+n)} \tag{2.22}$$

$$\alpha_x = -\frac{2}{\mathrm{kl}} - \frac{2}{l(k+l)}\frac{\varepsilon_r(i,j) - \varepsilon_r(i-1,j)}{\varepsilon_r(i,j) + \varepsilon_r(i-1,j)}$$

$$-\frac{2}{k(k+l)}\frac{\varepsilon_r(i,j) - \varepsilon_r(i+1,j)}{\varepsilon_r(i,j) + \varepsilon_r(i+1,j)}$$

$$= -\frac{4}{kl} + \alpha_k + \alpha_l \qquad (2.23)$$

$$\alpha_y = -\frac{2}{\mathrm{mn}} = -\alpha_m - \alpha_n \qquad (2.24)$$

Adjusting above equation for each mesh node of fiber gives an Eigen-value equation of the form as follows:

$$[M_{i,j}]\ E_x = (k_0\ n_{eff})^2\ E_x \qquad (2.25)$$

Here, $M_{i,j}$ is a Hermitian operator in which the indices i and j represent the arbitrary node points along x- and y- direction, respectively.

While calculating effective refractive index (β / k_0) from the matrix mentioned in Equation 2.25, we apply analytical boundary conditions in which field decays exponentially at the points of discontinuity of the structure. A mathematical expression for analytical boundary can be given as:

$$E_x(x,y) = K_0\sqrt{[|\beta|K_0 - \varepsilon(x))\Delta]}\ \ Ex(x\text{-}1,y) \qquad (2.26)$$

Implementation of the coding in Matlab software has been done as per the flow chart visible in Figure 2.2.

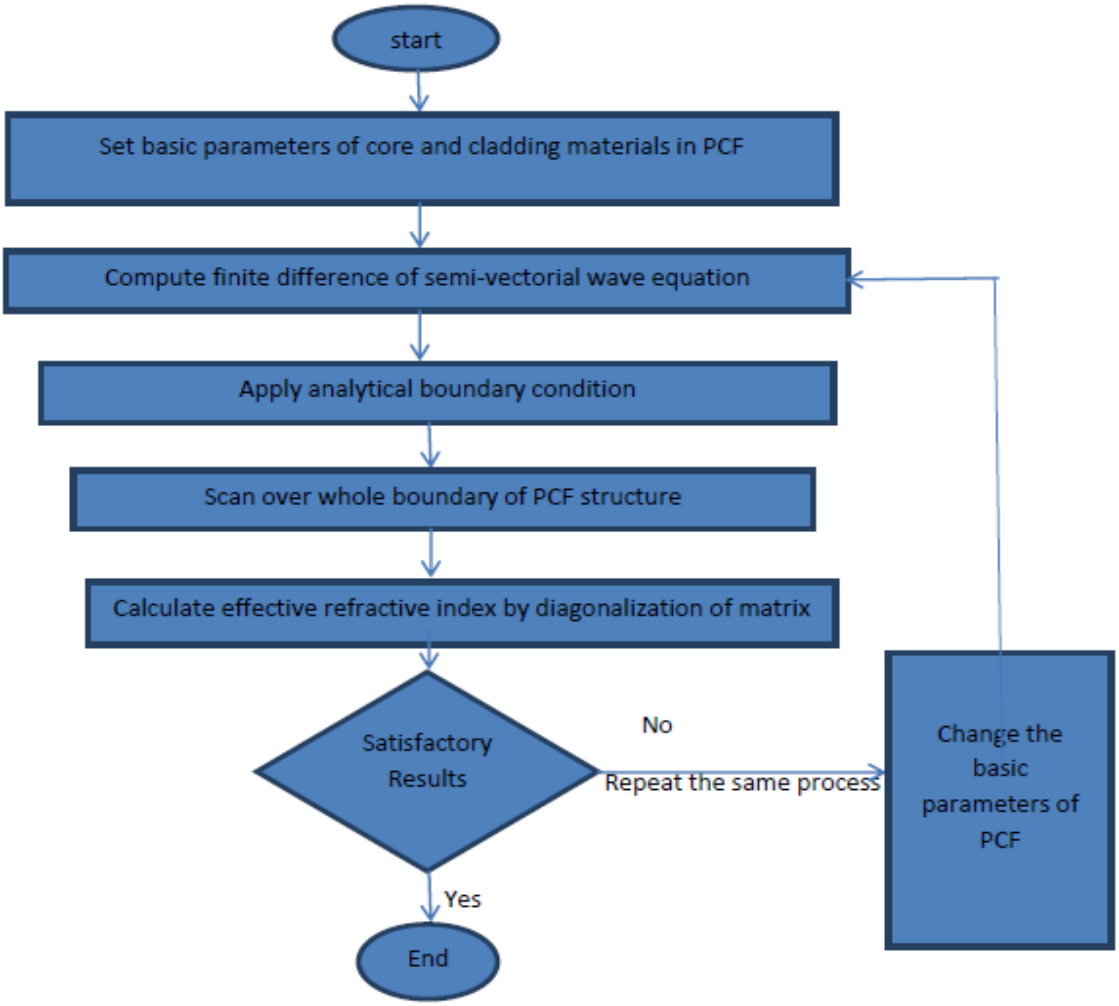

Figure 2.2 Flow chart to compute effective index of PCF.

We have calculated effective refractive index (n_{eff}) of PCF with the help of a frequency domain algorithm based on FDTD technique which is implemented in computational software, Matlab. Since our emphasis is on determining the values of dispersion, the effective index computed in our work is a measure of only the real part of the total effective index which in turn comprises of imaginary as well as real part. The effective index values of PCF are then deployed to calculate and plot dispersion curves.

$$D = -\frac{\lambda}{c}\frac{\partial^2(\mathrm{Re}[n_{eff}])}{\partial\lambda^2} \quad (2.27)$$

D in the Equation (2.27) is known as chromatic dispersion and is the sum of material as well as waveguide dispersion. The parameter c is the velocity of light in a vacuum, λ is the wavelength of the field propagating in the fiber and $Re(n_{eff})$ is the real part of the n_{eff}. The values of $Re(n_{eff})$ are same as that of n_{eff} evaluated in this paper. The waveguide dispersion can be calculated from similar equation, from which the chromatic dispersion is calculated whereas material dispersion is calculated from Sellmeir's formula.

The normalized frequency (V_{eff}) for any PCF can be evaluated from :

$$V_{eff} = \frac{2\pi}{\lambda}\Lambda\,(n_{co}^2 - n_{eff}^2)^{1/2} \quad (2.28)$$

In Equation (2.28), n_{co} and n_{eff} denote the refractive index of core and effective refractive index of the PCF respectively. The value of V_{eff} suggests the type of mode propagation in the PCF. The PCF can operate both in single mode as well as multimode condition for propagation of electromagnetic wave.

2.3 DESIGN GEOMETRY AND SIMULATION RESULTS

In our work a hexagonal lattice photonic crystal fiber is used for computation whose schematic cross-section is shown in Figure 2.3. The air holes are having a diameter (d), which is fixed at 1.8 μm. The separation between the center of two consecutive air holes, also known as pitch (Λ) is made equal to 2.3 μm. Four rings of air holes are embedded in the cladding of the PCF containing 6, 12, 18 and 24 air holes respectively starting from the center of the structure. The refractive index of each of the air holes is taken to be 1, as that of air.

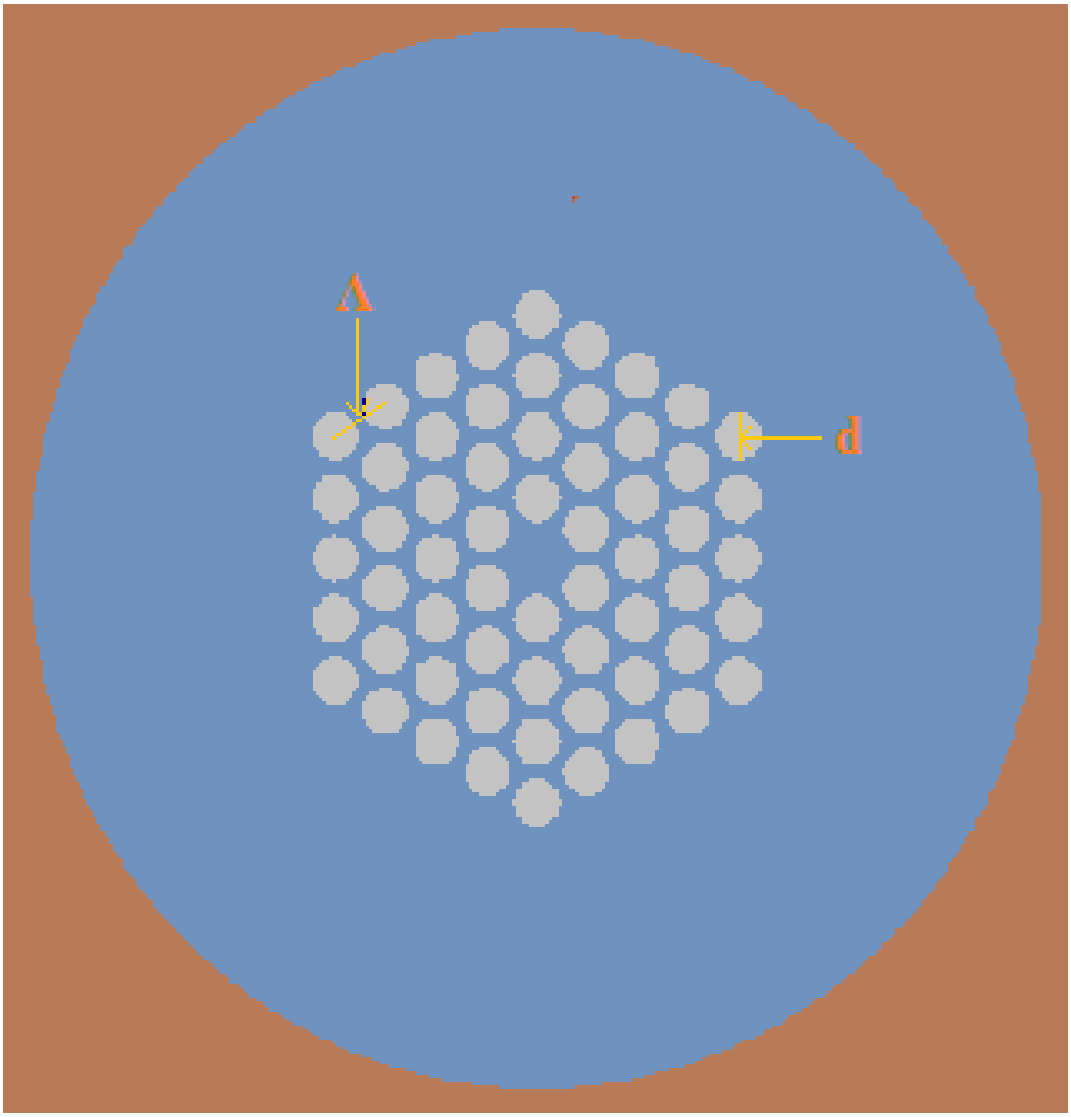

Figure 2.3 Hexagonal lattice photonic crystal fiber with 4 rings of air holes.

Excluding the air holes, whole PCF comprising of core and cladding is assumed to be made of pure silica which has a refractive index of 1.45. The diameter of the cladding of the PCF is set to be 40 μm in dimension, although this quantity has a minimal effect on the computation and can be ignored since the electromagnetic modes are confined only upto the air hole region in our case.

The new aspect of hexagonal lattice PCF which we have studied in this paper is the effect on dispersion values by changing the core's refractive index (n_{core}) or that of PCF otherwise. Instead of saying the refractive index of PCF we will use only the core's refractive index since the whole geometry of PCF is connected and the cladding region, leaving air holes is having the same refractive index as that of core. The refractive index of pure silica can be varied by doping of some impurity like Germanium, Gallium, Phosphorous etc. and then a preform can be made of the doped glass for using it to draw optical fiber via fiber drawing tower. We have varied the refractive index of core from 1.45 to 1.5 with an increasing order of 0.01 and plotted the dispersion curves for each value of refractive index. The dispersion curves are plotted by varying the ratio of diameter of air hole to the pitch (d/Λ) at each refractive index of core (n_{core}). The ratio of d/Λ is taken to be 0.78, 0.82 and 0.86 for each value of n_{core} and graphs have been plotted for the values of dispersion against wavelength. The wavelength band which is considered for finding out the values of effective index and thus dispersion parameters is taken to be S+C+L band which is used in telecommunication. As we can see in Figure 2.4, there is observed a negative dispersion for all the values of d/Λ for each refractive index of the core. Dispersion flattening is visible prominently for d/Λ=0.78 from 1.50 to 1.60 μm wavelength within a vertical range of 2.5 ps/nm-km only. We also notice from the above mentioned figure that as we increase the refractive index of core of PCF from 1.45 to 1.48, there is detected a downward shift in the dispersion curves. For every increment in the core's refractive index, the dispersion curves shift by about 10 ps/nm-km for the same value of d/Λ.

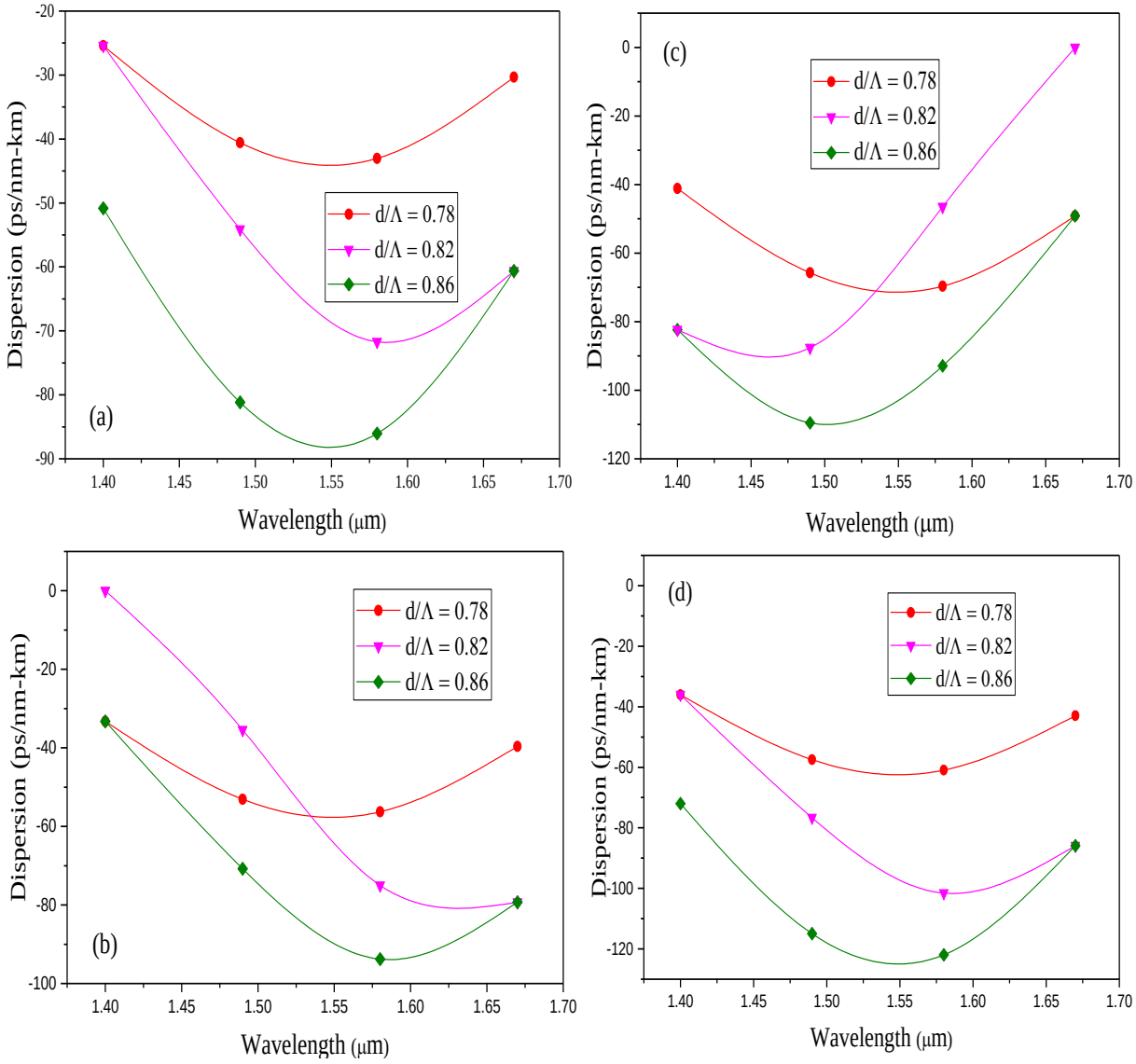

Figure 2.4 Dispersion properties of the hexagonal PCF as a function of wavelength with refractive index of core, n_{core}= (a) 1.45 (b) 1.46 (c) 1.47 (d) 1.48.

Normalized frequency (V_{eff}) of the PCF is calculated for all the four values of core's refractive index viz. 1.45, 1.46, 1.47 and 1.48 at d/Λ=0.82. The values of V_{eff} are plotted against wavelength in Figure 2.5.

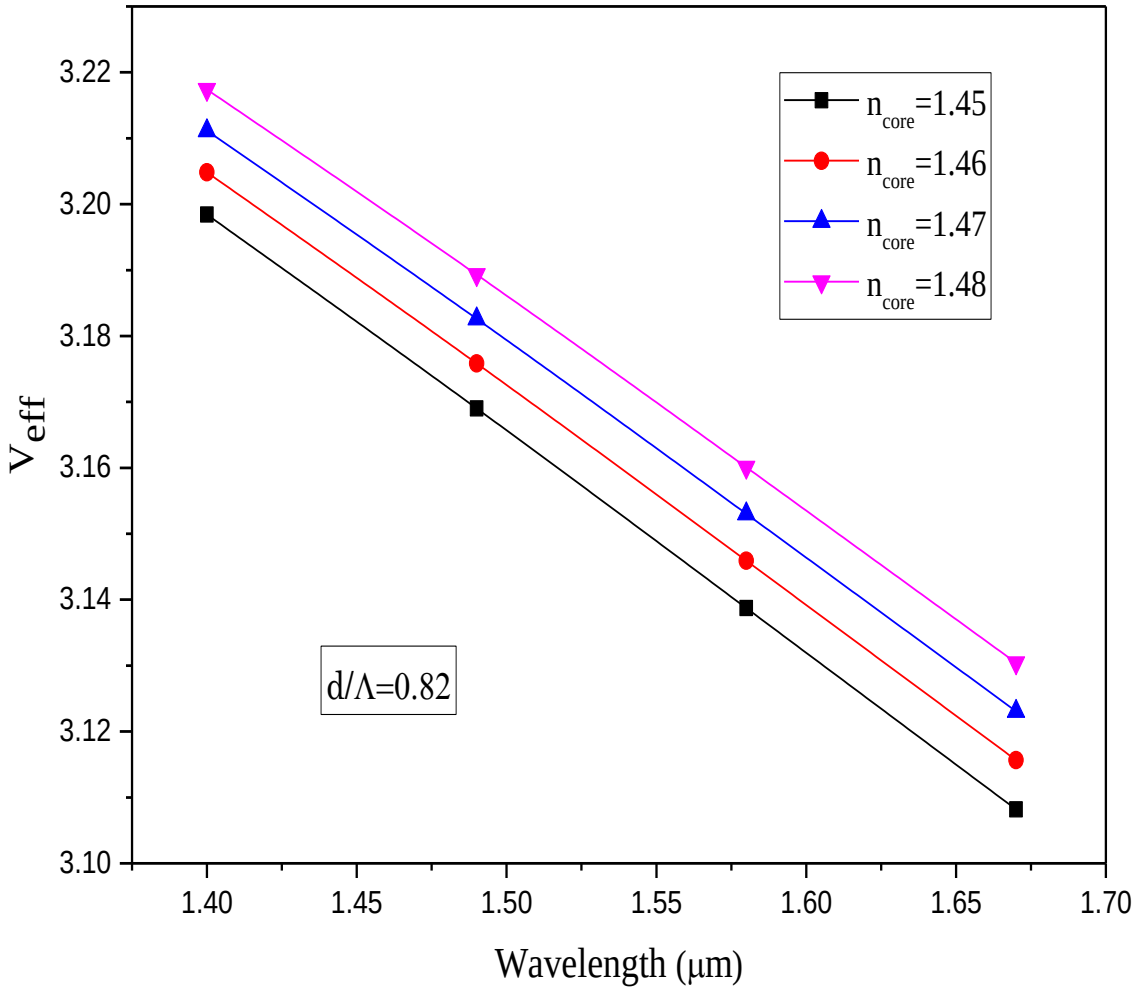

Figure 2.5 Wavelength dependence of V parameter value for d/Λ=0.82 and n_{core}=1.45, 1.46, 1.47 and 1.48.

As we can see from the figure, there is an increase in the values of V_{eff} with increase in the values of n_{core} at each wavelength in the S+C+L communication band. The curves

plotted between V_{eff} and wavelengths have a continuously decreasing slope. Also there is equal spacing between any two adjacent slopes of V_{eff}.

At last, a graph has been devised between the values of effective refractive index versus wavelength for polarized and scalar electric field for each refractive index of core. The solid lines in the Figure 2.6 are plotted by taking the input field as polarized in either X or Y direction, since the values of n_{eff} are same in any polarized condition for our structure. When the values of n_{eff} are plotted against wavelength for an unpolarized field or we can say for an electric field which is scalar then we get the curves as dashed lines visible in the same figure as referred to in the previous statement.

A field can transmit in a PCF either in a polarized manner or scalar (unpolarized) fashion. When the field's total intensity component is only in either X or Y direction then it is said to be polarized state. When the field's amplitude is independent of both the directions then that field is known to be propagating in scalar condition. The effective refractive index can be calculated for either polarized or scalar behaviour of the wave in the fiber.

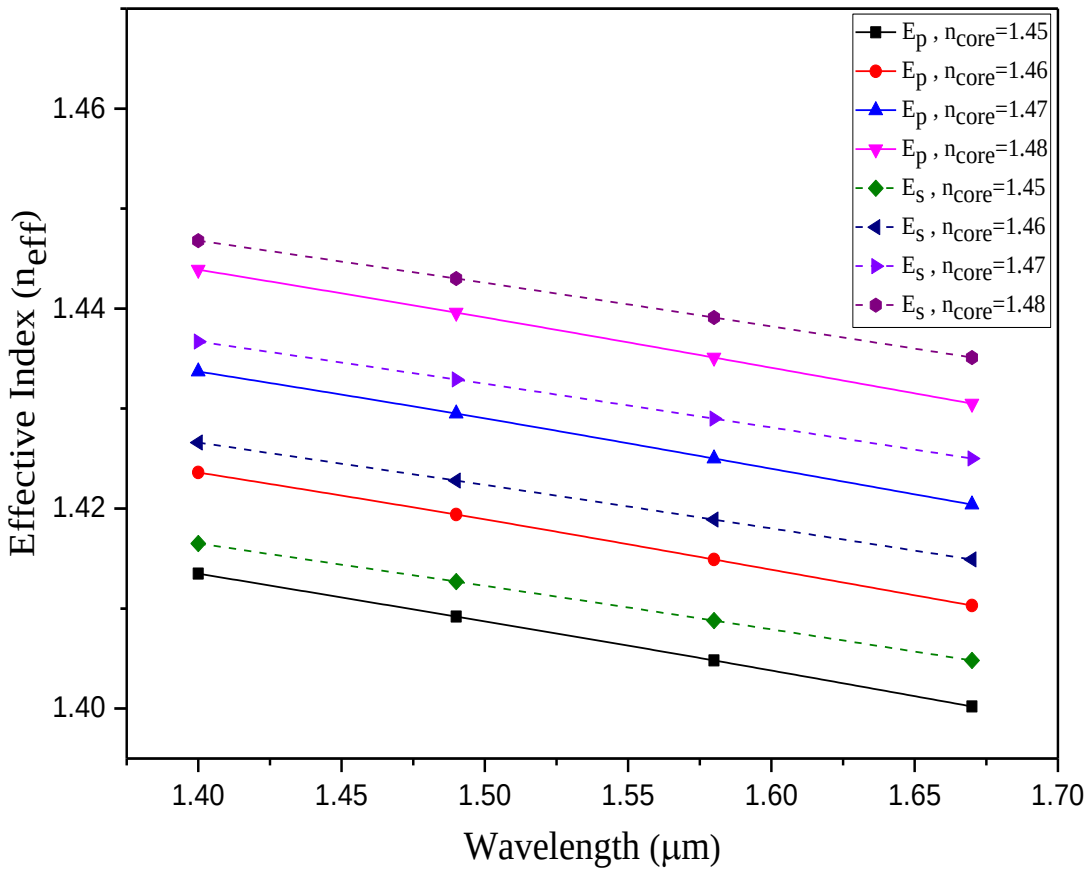

Figure 2.6 Effective index values of PCF plotted against wavelength in case of polarized as well as scalar input field represented by Ep and Es respectively at n_{core}= 1.45, 1.46, 1.47 and 1.48.

2.4 CONCLUSION

In conclusion, we report the simulation of a hexagonal lattice photonic crystal fiber by varying the refractive index of its core with the help of FDTD technique implemented in Matlab software. The results show that the dispersion increases in the negative direction with increase in the value of n_{core} of PCF, by an average amount of 10 ps/nm-km in S+C+L communication band. For a particular value of n_{core}, negative dispersion increases with

increase in d/Λ values in the same communication band. There is observed dispersion flattening between 1.50-1.60 μm wavelength for d/Λ =0.78 within a range of 2.5 ps/nm-km at each refractive index of core. The graph plotted between values of V_{eff} against wavelength suggests that there is a linear relationship between V_{eff} and wavelength and as we increase the n_{core} of PCF, the normalized frequency also increases with fixed steps. Lastly we have shown that the values of n_{eff} calculated in the case of scalar electric field are higher, than which are evaluated in the polarized field. For every n_{core} there is an equal jump in the values of n_{eff} in case of scalar field as compared to polarized one. This kind of PCF can be used in the applications such as dispersion flattening, dispersion compensation and band-pass or band-reject filters in optical communication systems. It has the potential to be used in multimode regime of wave propagation apart from single mode, thus making it to transfer more data at the same time. It can also act as polarization filter in optical networks by being able to detect scalar or polarized field one at a time.